MJ2412 Renewable Energy Technology
Morocco Proposal

Alexandre Oudet 930415-T096
Jean-François Olivier 921113-T116
Heinrich Boeing 890811-T431
Akshaya Kumar 940203-T083
James Buckland 940612-T054

March 17, 2015

Contents

List of Figures

1 Introduction

The Government of the Kingdom of Morocco has recently launched a program to increase the penetration of solar power in the national energy market. Thus, an contract has been promised to the independent energy production corporation able to deliver 100 MWe of base-load capacity from a concentrated solar power (CSP) plant to the grid at the lowest price.

At SolenKRAFT AB, our group of R&D Engineers has been appointed responsible for providing a suitable initial design to meet the required capacity and operating strategy. This report will present a technically viable solution, and clearly state the limitations and problems with the project. No cost estimation will be performed.

Of the different types of solar concentrators (presented in Figure 1) we consider those suitable for industrial use at medium to high power at temperatures of above 250°C. These devices use reflective surfaces to mirror sunlight, and are differentiable by their variable geometries. There are three types: *a*) parabolic trough, *b*) central tower, and *c*) parabolic-mirror CSP plants.

We choose the parabolic trough in order to meet our base-load capacity requirement of 100 MWe. In a parabolic trough, sunlight is concentrated towards a receiver carrying a heat transfer fluid. With water as the transfer fluid, steam is directly generated for use in a power plant. However, the stability of a water-based receiver is uncertain, and steam-based heat storage is complex. We thus propose the use of an oil-based fluid for heat transfer. These oils are single-phase fluids with an efficient heat transfer coefficient, and a temperature range fitting our needs, as well as the possibility for direct storage. Synthetic oils are preferred over mineral oils for their lesser flammability. We will employ this working fluid in a thermodynamic Rankine cycle, detailed in Section 4.

2 Location

The location of a CSP plant requires a direct normal irradiation of more than 1800 kWh/m^2, unprotected land, grade of less than 2%, and a stable soil basin. We also prefer proximity to a water source, as well as basic telecommunications, fuel pipelines, airports, and general infrastructure.

With these criteria in mind, a location 13 km from the city of Ouarzazate, Morocco was chosen, containing everything required for our power plant. It is 18km from the nearest body of water, and 14km from the nearest airport (`OZZ`). Details are presented in Figure 5.

The DNI was found using data from SoDa, a service that provides solar radiation data. The monthly direct normal irradiance was measured and averaged in order to calculate the annual DNI. Research was conducted and it was found that the Ait Oukrour Toundout, a local community, owns the region. Fortunately, the families of the community do not live in the area, but on the boundary of the protected area so no displacement of people will be necessary. Details are presented in FFigure 2.

3 Thermal Storage

With a TESh of 4 hours, we employ a production schema with 12 hours of sunlight-based electricity production, at a solar multiple of 1.33. This allows us to produce 16 hours of continuous baseline electricity. Using data representative of hourly power consumption

Figure 1: Attributes of Common Renewable Energy Power Plants

Technology	**Parabolic Trough**	**Tower**	**Parabolic**
Power Range	80-300 MW	10-100 MW	1-100 kW
Operating Temperature	270-450°C	450-1000°C	600-1200°C
Solar Field Cost	210-250€/m^2	140-220€/m^2	150€/m^2
Investment Cost	2.8-3.5€/We	3-4€/We	10-14€/We

Figure 2: Properties of CSP Site Location

Region	Souss-Massa-Draa Region; Ouarzazate
Latitude	31.027°N
Longigute	7.0035°W
Altitude	1901 m
Time Zone	GMT+0
Annual DNI	2204 kWh/m^2
Direct Irradiation[1]	495.10 W/m^2
Cosine Effectiveness N-S tracking[2]	0.9465
Approximate Land Size	9 km^2
Land Protection	No
Land Ownership	Ait Oukrour Toundout
Availability of Water	Yes
Distance to Source of Water	18km
Gas/Fuel pipeline	No
Telecom	Yes

Figure 3: Hourly Power Consumption in Morocco

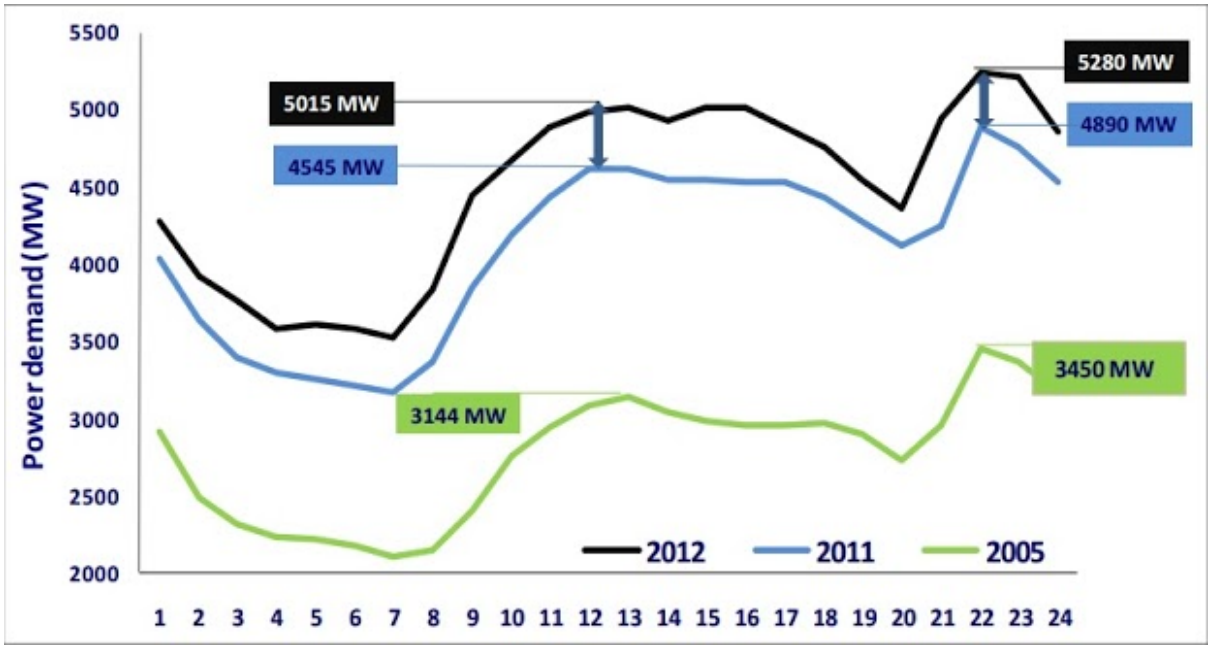

in Morocco (see Figure 3), we design a system which covers the peak hours of power demand in the region, from 08.00 to 24.00, with peaks at 12.00, 15.00, and 22.00, at small additional cost for the power required to store this energy. Thus, we can remain competitive after sunset without outpacing our reserves early in the day.

With obvious limitations on the amounts of available daylight, we choose not to run a 24hr production plant for its diminishing returns in the hours between 01.00 and 08.00, when demand is low and electricity prices cannot compensate for the additional energy stored since sunset.

4 Power Block

In order to calculate the mass flow required for our base load of 100 MWe, it is necessary first to design the power block. Here we present the main components of our prospective power block, still a generalised representation in our first draft. The turbine chosen for our reheat cycle is a Siemens SST-600, with output up to 150 MWe and inlet conditions of up to 165 bar / 565°C, with five bleeds and a reheat mode. We choose this turbine in order to deliver significantly greater than 100 MWe, accounting for parasitic losses. Additionally, its inlet conditions are a safety factor higher than necessary for our power block.

We also present a layout, as seen in Figure 4. To improve the efficiency of the steam cycle, we add a reheater, a feedwater tank, and a reheat cycle to our Rankine cycle. We also include a fossil fuel backup, to ensure the ability to produce and sell electricity even without optimal sunlight. Details are presented in Figure 5.

We use a Mollier Chart to obtain enthalpies, and calculate the mass flow in the steam cycle: $\dot{m}_{\text{total}} = 106kg/s$. This mass flow is required to reach 100 MWe of base load in the solar field. We then adapt the base load by increasing it to cover the electric power necessary to operate the pump. Our total mass flow in the solar field $\dot{m}_{\text{solar}} = 1475kg/s$ delivers an initial power of 325 MW to the boiler, which produces the optimised and reasonable global power block efficiency of $\eta_{\text{total}} = 32\%$.

This slightly subpar efficiency comes at the benefit of a guaranteed revenue by way of reduced economic risk: by including backup and energy-saving measures in the design of our power block, we sacrifice some production-hours for a constant energy production capability. Additionally, this predictable, dispatchable electricity generation system ensures a simplified control schema for the power plant, with combustion-based control, and backup gas-fired boilers when steam temperature is at suboptimal temperatures. These multiple safety features ensure economic profitability in all weather conditions.

5 Solar Field Design

Of the many design options available for the Solar Collector Assembly (SCA),[3] the most common one is the Euro Trough System (ET), the first available standardised design on the market. We similarly considered the Helios (HT) and Ultimate Trough (UT) systems, each extensions of the ET. The UT and HT systems have better optical performance than the ET, and the UT system has the lowest costs.[4] Thus the UT system is chosen for this project.

We further detail the characteristics of our trough system and SCA. The basic characteristics: $l_{\text{ltrough}}, w_{\text{tr}}, l_{\text{sp}}, l_{\text{focus}}, A_{\text{SCA}}$, etc. are provided by the manufacturer.[5]

Figure 4: Power Block Schematic

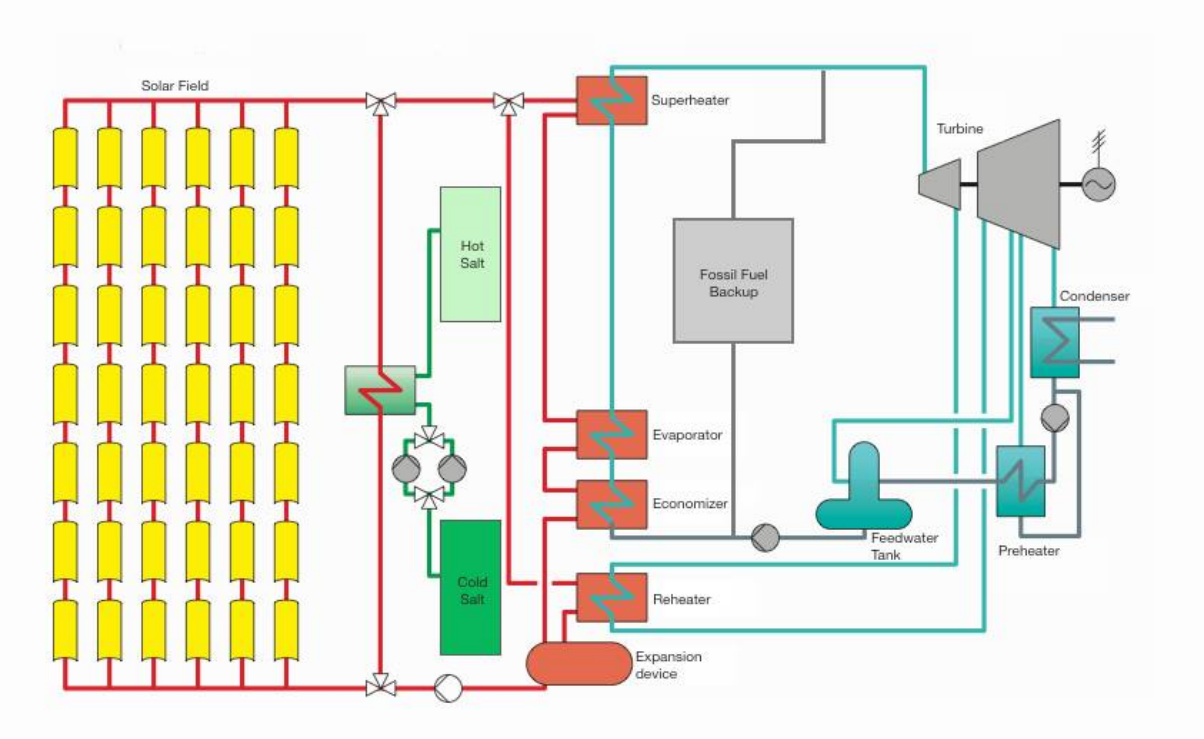

Figure 5: Properties of Power Block

Property	Value	Property	Value
Inlet temperature HP turbine	380°C	Inlet temperature boiler SF	400°C
Inlet pressure HP turbine	100 bar	Outlet temperature boiler SF	300°C
Inlet temperature LP turbine	380°C	Water temperature after preheater	100°C
Inlet pressure LP turbine	17 bar	Isentropic efficiency turbine	80%
Extraction pressure FWT	6 bar	Mechanical efficiency	98%
Extraction pressure preheater	1.5 bar	Generator efficiency	97%
Outlet pressure LP turbine	0.1 bar	Heat exchanger SF/boiler efficiency	93%

Due to a lack of agreement in the literature, we calculate the incidence angle modifier (IAM) as described in Equation 1. [6]

$$\text{IAM} = \max\left[0, (1 + a_1\sigma_t + a_2\sigma_t^2)\right] \tag{1}$$

The UT system employs RP5 mirrors,[7] with mirror reflectivity factor $p_{\text{ref}} = 0.945$.[8] We assume a reasonable cleanliness factor $f_{\text{clean}} = 0.95$, despite the highly exposed Saharan location. An automatic cleaning system, common in the industry, is used to keep an acceptable level of cleanliness.[9]

We determine the length between two rows of SCA with an optimisation iteration. Higher values of l_{sp} lower the shadowing effect, but increase the thermal and friction losses of the pipes (estimated at around 300 W/m)[10] necessary to connect the SCAs. Estimating a value of l_{sp} between 6 m and 15 m, an optimisation method finds 8.4 m ideal, with trough characteristics presented in Figure 6.

Information derived from location characteristics, presented in Figure 2, recommend a N-S tracking system, with optimal cosine effectiveness. We similarly calculate all relevant figures relative to the power output of one SCA, presented in Figure 7. The incidence angle and the irradiance are mean values for the 21st day of every month in 2005. The values and calculations can be found in Appendix C.

$$Q = A_{\text{SCA}}\ I\ e_{\text{surf}}\ e_{\text{cos}}\ \text{IAM}\ (1 - f_{\text{shd}})\ (1 - f_{\text{end}}) = 655.66\ \text{kW} \tag{2}$$

Thus the power output of a single SCA is presented in Equation 2.

We present a tentative layout for a solar field in Figures 8 and 9. The length of a single loop is determined by optimisation between pressure losses, practical mass flow, and the necessary length of a piping system. Longer loops require higher mass flows and higher pressure losses, but shorter loops require a complex field layout with longer piping systems, which also increase pressure losses. We choose an optimal loop length of 4 SCAs, with dimensions detailed in Figures 8 and 9.

6 Receiver Selection

For this solar field, we employ the Schott PTR®70 Receiver,[11] a tubular receiver carrying Therminol VP-1,[12] a synthetic liquid/vapour fluid specifically designed for ultra-high temperature heat transfer. The receiver has dimensions and specifications as stated in Figure 10.[13] At an estimated average operating temperature of 350°C, this fluid has a heat capacity 2.4606 kJ/kg.K, a density of 758.247 kg/m^3, and a dynamic viscosity of 1.77e-03 Pa.s (see Appendix A for derivational details). The localized friction factor, viscosity, and temperature differences have all been included in a calculation of pressure and energy losses over the piping system.

We chose the Schott PTR®70 Receiver as a standard-issue solar receiver, employed in many other existing and profitable solar power plants around the world.[14] The receiver is rated at up to 400°C, and has been ranked by testing at DLR (the German Aerosopace Centre) as the premier solar receiver currently on the market. The working fluid, Therminol VP-1, is also an industry standard, in use in concentrated solar power plants since the 1980s. We believe these two standards to be the most economically safe and technically reliable products on the market.

Figure 6: Characteristics of the UT System

Trough Characteristics	Value
l_{trough}	242m
w_{tr}	7.5m
l_{sp}	8.3m
l_{focus}	1.95 m
A_{SCA}	1689 m^2
p_{ref}	0.945
f_{clean}	0.95
f_{end}	0.003
f_{shd}	0.012
a_1	0.00010596
a_2	0.00017091

Figure 7: Relevant Power Output Characteristics

Output Characteristics	Value
ϵ_{surf}	0.8979
ϵ_{cos}	0.9465
θ	18.82°
I_0	495.10 W/m^2
IAM	0.9367
f_{end}	0.003
f_{shd}	0.012
A_{SCA}	1689 m^2

Figure 8: Solar Field Macro View

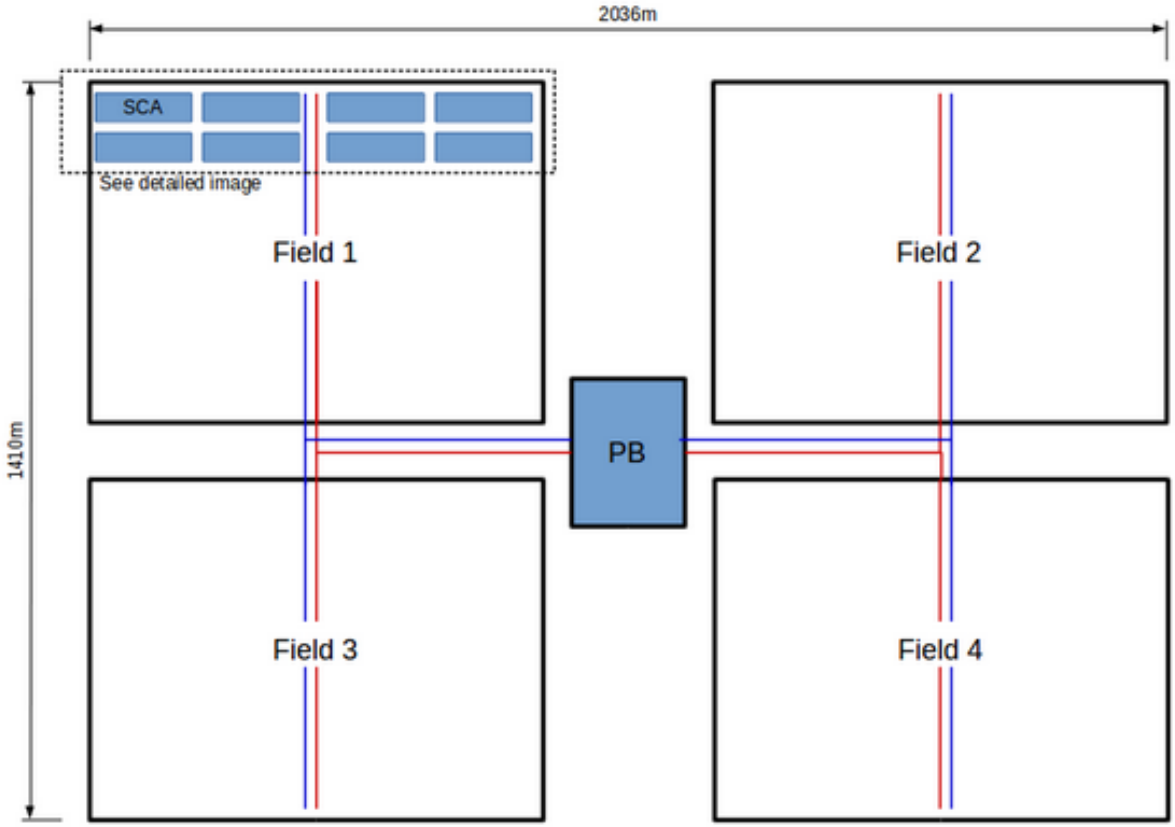

Figure 9: Solar Field Micro View

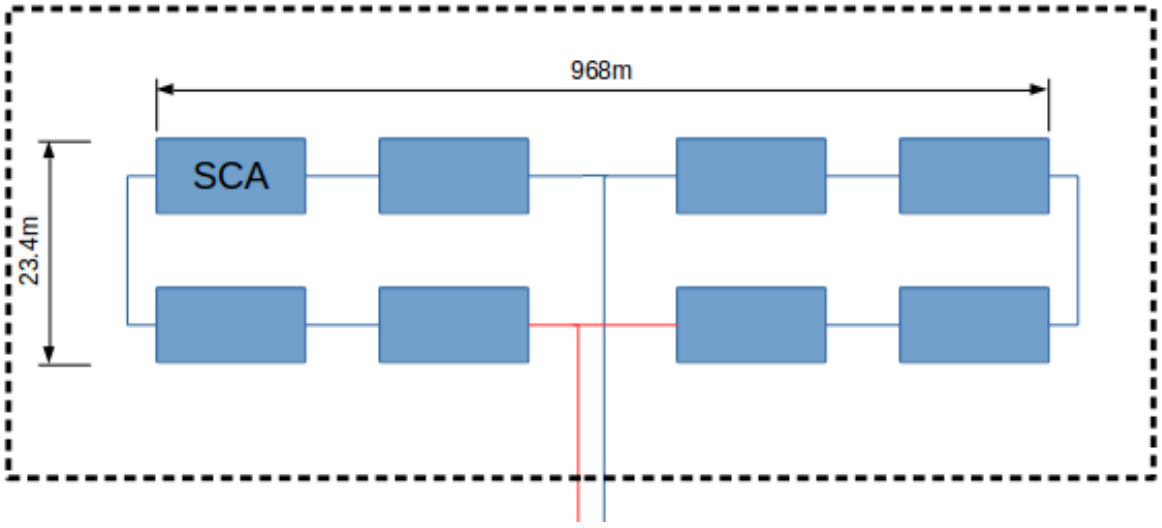

Figure 10: Characteristics of the Receiver System

Dimensions	Length	4060 mm
	Outer Diameter	125 mm
Absorber	Outer Diameter	70 mm
	Steel Type	DIN 1.4541
	Thermal Emittance	$\epsilon \leq 9.5\%$
	Solar Transmittance	$\tau \geq 97\%$
Thermal Losses	at 350°C	≤ 165 W/m
Operating Conditions	Pressure	≤ 41 bar absolute

7 Iteration Methods

The design of a power plant is a complex process with hundreds of values variables, many of them circularly dependent on each other. One way to solve this problem is an iterative computational method of determination. This means introducing estimations for many numbers, and then having a computer iterate through their refinement and optimisation, with a particular goal in mind – in this case, the reduction of wasted power, the power required to maintain the plant.

Assuming a desired electrical power output of $P_{\text{desired}} = 100$ MWe, we introduce the a parasitic power P_{par}, with a total energy output of $\Sigma P = P_{\text{desired}} + P_{\text{par}}$. We introduce a best-case desire parasitic power, denoted as P^*_{par}.

We then incorporate realistic design estimates for the surface area, irradiance, etc. of a localised individual trough loop, which runs through six troughs. This allows us to calculate the power produced by a single loop, $P_{\text{SF}_{\text{loop}}}$. We also estimate the receiver losses per meter, which obtains the energy lost per loop, $P_{\text{loss}_{\text{loop}}}$. Assuming some reasonable thermally stored energy, $P_{\text{thermal storage}}$, we find the number of required loops, n_{loop}:

$$n_{\text{loop}} \times (P_{\text{SF}_{\text{loop}}} - P_{\text{loss}_{\text{loop}}}) = P_{\text{PB}} + P_{\text{thermal storage}}$$

From similar design estimates, we include pressure losses and the energy required to recoup these losses, which results in the real parastic power P_{par}. We scale this factor 150% to account for the estimated additional pressure and efficiency losses to pumps, joints, bends, and other pipe friction.

In the iteration step, we test to see if this calculated parasitic power P_{par} is close enough to the desired parasitic power P^*_{par}. If the values are too far apart, we make a better guess for the desired parasitic power, and re-iterate. Eventually the values converge, and we end up with not only a parasitic power with a physical basis, but the physical constants required to make the plant work at that efficiency as well.

8 Solar Multiple

The solar multiple of a solar power plant is the ratio of the actual power of the solar field for the design point and the power required to the power block to meet the rated power. Our solar field is oversized in order to produce and store thermal energy for after-hours production, and to compensate for a best-case scenario design, in which values are calculated at noons and solstices, when the solar flux is at its highest. Additionally, the Solar Multiple, unlike many other variables in the project, depends on the economic circumstances of the region, and the price at which it is competitive and realistic to

sell electricity. However, the technology required to capture, store, and return power is expensive proportional to the amount of energy stored. This thermal storage size h, has units of hours, as in hours of stored electricity. Thus, the desired solar multiple both a) *minimises* the levelized cost of electricity for the region (LCOE) and b) *minimises* the cost of storage. As we increase the size of the solar field, we produce more electricity and sell it for more profit. But at a certain point the cost required to store and maintain a solar field and thermal reserve outpaces the profit made from the sale of electricity.

Thus, to solve this problem in an iterative fashion we create a two-dimensional function of the LCOE as a function of the solar multiple and the thermal storage size. However, without the proper economic resources and data for a technically correct LCOE calculation, we merely include the iterative mechanism in our spreadsheet, and assume a fairly standard solar multiple of 1.3 in our calculations. This is enough to provide an additional four hours of electricity for every twelve spent in sunlight.

Notes

[1]See Section 4 for calculations of mean direct irradiation and cosine effectiveness.

[2]Calculated at mean values per month, valid in the year 2005.

[3]If not indicated differently, the following assumptions and calculations are based on the lecture Renewable Energy Technologies (MJ2412) at KTH-ITM. We assume that the reader of this report is familiar with the lecture and hence do not display it here in further detail.

[4]`http://elib.dlr.de/79213/1/Thermodynamic_simulation_of_solar_thermal_power_stations_with_liquid_salt_as_heat_transfer_fluid_Patrick_Wagner.pdf`, p.8

[5]`http://elib.dlr.de/79213/1/Thermodynamic_simulation_of_solar_thermal_power_stations_with_liquid_salt_as_heat_transfer_fluid_Patrick_Wagner.pdf`, p.113 and `http://www.flabeg-fe.com/en/engineering/ultimate-trough.html`

[6]`http://elib.dlr.de/79213/1/Thermodynamic_simulation_of_solar_thermal_power_stations_with_liquid_salt_as_heat_transfer_fluid_Patrick_Wagner.pdf`, p.57 gives an idea of the IAM. Nonetheless the real IAM of the Ultimate Trough system is not available at this time.

[7]`http://social.csptoday.com/sites/default/files/4aFLABEG.pdf`, p.15.

[8]`http://www.flabeg-fe.com/uploads/media/FLABEG-FE-parabolic-trough-mirrors.pdf`

[9]`http://sfera.sollab.eu/downloads/Schools/Reflector_Soiling_Fabian_Wolfertstetter_SFERA2013.pdf`

[10]This figure is an assumption based on the first iteration of the design of the solar field and is subject to change.

[11]`http://www.schott.com/csp/english/schott-solar-ptr-70-receivers.html?so=scandinavia&lang=english`

[12]`http://twt.mpei.ac.ru/tthb/hedh/htf-vp1.pdf`

[13]`http://www.schott.com/csp/english/download/schott_ptr70_4th_generation_datasheet.pdf`

[14]`http://www.therminol.com/applications/concentrated-solar-power`

A Properties Calculation for Therminol VP-1

A.1 Heat Capacity

As obtained from the *Therminol VP-1* datasheet [15], the heat capacity of Therminol VP-1 can be expressed as a function $C(t)$ of the operating temperature:

$$\begin{aligned} H(t) = \text{Heat Capacity (kJ/kg.K)} = &+ 0.002414 \times T(^\circ C) \\ &+ 5.9591 \times 10^{-6} \times (T(^\circ C))^2 - 2.9879 \times 10^{-8} \times (T(^\circ C))^3 \\ &+ 4.4172 \times 10^{-11} \times (T(^\circ C))^4 + 1.498 \end{aligned}$$

The receiver discussed in Section 6 has an operating temperature of between $300^\circ C$ and $400^\circ C$, with an average of $350^\circ C$. It follows that the heat capacity will not be the value of the heat capacity function at the average value, but rather the average of the function across the range of values. We thus integrate the above function between 300 and 400:

$$\frac{1}{(400^\circ C) - (300^\circ C)} \int_{300^\circ C}^{400^\circ C} H(t)\ dt = \boxed{2.4606 \text{ kJ/kg.K}}$$

This calculation seems trivial without the understanding that the heat capacity of the working fluid directly impacts the parasitic power, and therefore the LCOE for the entire project.

A.2 Density

We repeat the above for the density of the fluid:

$$\begin{aligned} \rho(t) = \text{Density}(\text{kg/m}^3) = &- 0.90797 \times T(^\circ C) + 0.00078116 \times (T(^\circ C))^2 \\ &- 2.367 \times 10^{-6} \times (T(^\circ C))^3 + 1083.25 \end{aligned}$$

$$\frac{1}{(400^\circ C) - (300^\circ C)} \int_{300^\circ C}^{400^\circ C} \rho(t)\ dt = \boxed{758.247 \text{ kg/m}^3}$$

B Calculated Design Values

The calculated design variables of our final iteration are presented in Figure 11. Because of the iterative nature of our project, a single change of measurement will have repercussions throughout the project. While we attach Figure 11 for reference (i.e. for scale, size estimates, and sanity checks), any edits or experiments should be run on the actual spreadsheet, which we have attached for convenience.

C Solar Energy Calculations

To get accurate values for the solar irradiance and other geometrically-influenced constants, we used data taken from the 21st of each month throughout a given year (in this case, 2005) and then took the weighted average. The raw calculation tables can be found in Figure 12, and were derived using the equations in Figure 5 for at coordinates (31.03°N, 7.00°W), UTC+0.

Figure 11: Calculated Design Values

description	var	value	units
Power Block			
estimated parasitic power	P^*_{par}	2.811	MW
power block efficiency	η_{pb}	0.32	-
power needed in power block	Q_{pb}	321.28	MW
Solar Field			
area of one loop	A_{loop}	7578	m^2
local irradiance	I_0	495.1	W/m^2
surface cleanliness factor	ϵ_{surf}	0.8978	-
cosine efficiency	ϵ_{cos}	0.9465	-
incidence angle modifier	IAM	0.9367	-
shadowing factor	f_{sh}	0.988	-
end factor	f_{end}	0.997	-
Reciever			
losses per meter	q	150	W/m
length of one loop	l_{loop}	1085.83	m
Pressure Losses			
thermal capacity of oil	c_p	2460	kJ/kg.K
change in temperature	ΔT	100	K
mass flow through loop	$\dot{m}_{\text{loop}}$	11.96	kg/s
diameter of tube	d_i	0.07	m
cross-sectional area	A	0.0038	m^2
dynamic viscosity	μ	1.77×10^{-3}	Pa.s
density of fluid	ρ	758	kg/m^3
flow rate of loop	$\dot{v}_{\text{loop}}$	0.016	$\text{m}^3\text{/s}$
velocity of fluid	v	4.10	m/s
local reynolds number	Re	1.23×10^5	-
friction factor	f	5.18×10^{-3}	-
Additional Factors			
total mass flow	$\dot{m}$	2080.72	kg/s
size of thermal energy storage (in hours)	TES_{h}	6.00	hours
(in MWh)	TES_{th}	1927.70	MWh
average day length	Δt	12	hours
required additional energy	E_{add}	160.6	MW
total energy of solar field	ΣQ_{SF}	2.94	MW
number of loops	n_{loop}	174	-
max temperature	T_{max}	400	°C
min temperature	T_{min}	300	°C
energy loss per loop	Q_{loss}	0.16	MW
change in pressure	Δp	89.1	MPa
real parasitic power	P_{par}	2.8	MW

Figure 12: Solar Energy Values

Month	Date	n	T_{EOT}	T_s	w	δ	θ_z	γ_s	θ_t
			minutes	hours	radians	radians	radians	radians	radians
January	21	21	-10,94	11,35	-0,17	-0,35	0,91	0,98	0,45
February	21	52	-13,94	11,30	-0,18	-0,20	0,76	0,97	0,40
March	21	81	-7,34	11,41	-0,15	-0,01	0,57	0,96	0,31
April	21	112	1,56	12,56	0,15	0,20	0,37	0,92	0,22
May	21	142	3,57	12,59	0,16	0,35	0,24	0,79	0,17
June	21	173	-1,74	12,50	0,13	0,41	0,18	0,73	0,13
July	21	203	-6,40	12,43	0,11	0,35	0,21	0,87	0,14
August	21	234	-2,99	12,48	0,13	0,20	0,36	0,94	0,21
September	21	264	7,31	12,65	0,17	0,00	0,56	0,95	0,32
October	21	295	15,78	12,80	0,21	-0,20	0,77	0,96	0,41
November	21	325	13,54	11,76	-0,06	-0,35	0,90	1,00	0,44
December	21	356	1,21	11,55	-0,12	-0,41	0,96	0,99	0,46

Figure 13: Solar Equations

$$
\begin{aligned}
t_s &= t_{\text{clock}} + \frac{\Psi_{\text{std}} - \Psi_{\text{loc}}}{15^\circ} + \frac{\Delta t_{\text{EOT}}}{60} + \Delta t_{\text{DST}} \\
\Delta t_{\text{EOT}} &= 0.258 \cos\left(2\pi \frac{n-1}{365}\right) - 7.416 \sin\left(2\pi \frac{n-1}{365}\right) \\
&\quad - 3.648 \cos\left(4\pi \frac{n-1}{365}\right) - 9.228 \sin\left(4\pi \frac{n-1}{365}\right) \\
\omega &= \frac{\pi}{12}(t_s - 12) \\
\delta &= \arcsin\left(0.39795 \cos\left(2\pi \frac{n-173}{365}\right)\right) \\
N &= \frac{24}{N} \arccos(-\tan\phi \tan\delta) \\
\theta_z &= \arccos(\cos\phi \cos\delta \cos\omega + \sin\phi \sin\delta) \\
\gamma_s &= \text{sgn}(\omega) \left| \arccos\left(\frac{\cos\theta_z \sin\phi - \sin\delta}{\sin\theta_z \cos\phi}\right) \right| \\
\theta_s &= \frac{\pi}{2} - \theta_z
\end{aligned}
$$